



Feeder Power Disaggregation: A Data-Efficient Matrix Completion Approach

Preprint

Yue Chen, Ahmed Zamzam, and Andrey Bernstein

National Renewable Energy Laboratory

*Presented at the 2023 IEEE Power and Energy Society General Meeting
Orlando, Florida
July 16–20, 2023*

**NREL is a national laboratory of the U.S. Department of Energy
Office of Energy Efficiency & Renewable Energy
Operated by the Alliance for Sustainable Energy, LLC**

This report is available at no cost from the National Renewable Energy Laboratory (NREL) at www.nrel.gov/publications.

Contract No. DE-AC36-08GO28308

Conference Paper
NREL/CP-5D00-84138
July 2023



Feeder Power Disaggregation: A Data-Efficient Matrix Completion Approach

Preprint

Yue Chen, Ahmed Zamzam, and Andrey Bernstein

National Renewable Energy Laboratory

Suggested Citation

Chen, Yue, Ahmed Zamzam, and Andrey Bernstein. 2023. *Feeder Power Disaggregation: A Data-Efficient Matrix Completion Approach: Preprint*. Golden, CO: National Renewable Energy Laboratory. NREL/CP-5D00-84138. <https://www.nrel.gov/docs/fy23osti/84138.pdf>.

© 2023 IEEE. Personal use of this material is permitted. Permission from IEEE must be obtained for all other uses, in any current or future media, including reprinting/republishing this material for advertising or promotional purposes, creating new collective works, for resale or redistribution to servers or lists, or reuse of any copyrighted component of this work in other works.

**NREL is a national laboratory of the U.S. Department of Energy
Office of Energy Efficiency & Renewable Energy
Operated by the Alliance for Sustainable Energy, LLC**

This report is available at no cost from the National Renewable Energy Laboratory (NREL) at www.nrel.gov/publications.

Contract No. DE-AC36-08GO28308

Conference Paper
NREL/CP-5D00-84138
July 2023

National Renewable Energy Laboratory
15013 Denver West Parkway
Golden, CO 80401
303-275-3000 • www.nrel.gov

NOTICE

This work was authored in part by the National Renewable Energy Laboratory, operated by Alliance for Sustainable Energy, LLC, for the U.S. Department of Energy (DOE) under Contract No. DE-AC36-08GO28308. Funding provided by U.S. Department of Energy Office of Electricity under the Sensors and Data Analytics Program. The views expressed herein do not necessarily represent the views of the DOE or the U.S. Government.

This report is available at no cost from the National Renewable Energy Laboratory (NREL) at www.nrel.gov/publications.

U.S. Department of Energy (DOE) reports produced after 1991 and a growing number of pre-1991 documents are available free via www.osti.gov.

Cover Photos by Dennis Schroeder: (clockwise, left to right) NREL 51934, NREL 45897, NREL 42160, NREL 45891, NREL 48097, NREL 46526.

NREL prints on paper that contains recycled content.

Feeder Power Disaggregation: A Data-Efficient Matrix Completion Approach

Yue Chen, Ahmed Zamzam, and Andrey Bernstein
Power Systems Engineering Center
National Renewable Energy Laboratory
Golden, CO, USA.

Abstract—This paper presents a data-driven algorithm for the feeder power disaggregation problem in distribution systems. Leveraging spatio-temporal power patterns in residential homes, residential power is decomposed into three components: sparse-switching loads, periodic loads, and photovoltaic (PV) generation, which are characterized through the design of two sparse matrices and a low-rank matrix. The matrix completion process is data-efficient because of the matrix sparsity and low rankness, along with the use of power system models. The proposed approach is tested using real-world residential datasets on a 33-bus distribution system, demonstrating accurate power disaggregation with efficient matrix completion.

I. INTRODUCTION

The growing deployment of sensing facilities is producing enormous data for the modern power system. At the feeder level, phasor measurement units (PMUs) collect electrical phasor quantity (such as voltage or current) with a high temporal resolution close to system frequency, i.e., 60 Hz. Meanwhile, smart meters are widely installed in residential homes to provide the home-level power demand/generation with intervals of 15 minutes to an hour. These measurements offer various opportunities to improve the power system observability through data-driven approaches.

This work concerns the feeder-level power disaggregation problem that recovers specific power consumption/generation components from the feeder head power. Power disaggregation is valuable for grid operators to analyze the power demand/generation patterns in residential homes. With FERC order 2222 removing barriers for distributed energy resources to participate in energy markets, it is critical for system operators to characterize and forecast the flexibility from the aggregated resources within the feeder. In addition, understanding the breakdown of energy trajectories will improve the power system reliability and economic efficiency through effective system planning and operation.

This work was authored by the National Renewable Energy Laboratory, operated by Alliance for Sustainable Energy, LLC, for the U.S. Department of Energy (DOE) under Contract No. DE-AC36-08GO28308. Funding provided by U.S. Department of Energy Office of Electricity under the Sensors and Data Analytics Program. The views expressed in the article do not necessarily represent the views of the DOE or the U.S. Government. The U.S. Government retains and the publisher, by accepting the article for publication, acknowledges that the U.S. Government retains a nonexclusive, paid-up, irrevocable, worldwide license to publish or reproduce the published form of this work, or allow others to do so, for U.S. Government purposes. {yue.chen, ahmed.zamzam, andrey.bernstein}@nrel.gov.

In this paper, we consider a distribution system consists of the following types of energy resources: 1) loads that switch infrequently, such as electric vehicle batteries, washing machines, and kitchen ovens; 2) periodic loads that switch periodically, such as water heaters and refrigerators; and 3) residential PV power generation that share the similar solar irradiance within a feeder. According to these spatial-temporal characteristics, we develop three model structures to capture home power activities: a sparse matrix to recover sparse-switching loads (Section III-A); a sparse matrix with the basis of periodic waves to recover periodic loads (Section III-B); and a rank-one matrix to approximate the PV power in homes (Section III-C). However, performing direct feeder-head power disaggregation is challenging because the aforementioned home power characteristics are smoothed out after power aggregation at the feeder head. Therefore, we first disaggregate the power at the home level, then determine the corresponding power components at the feeder head using power flow models.

To achieve high-resolution feeder-level power disaggregation results, we consider two data sources: PMUs and smart meters. PMUs provide high-resolution measurements of feeder head power and voltage but only available at limited feeder nodes. Smart meters provide low-resolution home power but are widely deployed in residential homes. These two datasets, obtained with different temporal resolutions and spatial availability, are integrated to enhance system observability.

In the literature, the problem of non-intrusive load monitoring has been extensively tackled, e.g., [1]–[4] and the survey work [5]. Most relevant to this paper is the approach of [3] which disaggregates home-level power consumption into two main components, but it exhibits difficulties dealing with periodic loads. In paper [6], the independent component analysis (ICA) method, that widely used for blind source separation problems, is applied to disaggregate the heat, ventilation, and air-conditioning (HVAC) load using smart meter data. However, these work does not consider the disaggregation of feeder-level power trajectories, which is the focus of this paper. Related feeder-level power disaggregation literature includes [7]–[11] and their references. [7] uses multiple linear regression to disaggregate the solar power component from substation power measurements. [8] develops online power disaggregation algorithms with a focus on the aggregate air conditioners demand. While most work in the literature fo-

cuses on recovering a specific component of interest, e.g., air conditioners or solar, our work aims to recover all components in a distribution system. In addition, some works employ the artificial intelligence for power disaggregation. Papers [9], [10] use artificial neural networks with substation power and voltage measurements to disaggregate loads based on voltage-dependent characteristics. [11] applies multi-quantile recurrent neural networks for feeder-level power disaggregation, using feeder measurements, meteorological measurements, and calendar information. Unlike our data-efficient approach, these neural network-based approaches require big and rich training data that usually generated from simulations.

The contributions of this paper are summarized below: 1) we integrate smart meter and PMU data for enhanced system observability; 2) we formulate an efficient matrix completion problem for feeder-level power disaggregation, leveraging both system measurements and physical models; 3) we obtain high-resolution power disaggregation results at both home and feeder-head levels; 4) we illustrate the algorithm efficacy on the 33-bus distribution system with real-world load datasets.

The rest of the paper is organized as follows. Sections II and III discuss the system data and physical models employed in the power disaggregation problem, which then is formulated next in Section IV. Numerical results are presented in Section V. Conclusion and future work are given in Section VI.

II. DISTRIBUTION SYSTEM

Consider a balanced distribution system that connects a set of nodes $\mathcal{N} = \{0, \dots, N\}$, where node 0 is the feeder head with a fixed voltage v_0 ; the rest are PQ nodes that serve residential homes. The home power matrix is denoted as

$$\Omega := \begin{bmatrix} P \\ Q \end{bmatrix} \in \mathbb{R}^{2N \times T} \quad (1)$$

where P and Q represent the real and reactive power injections at N nodes for T discrete time.

In this work, we use two PMU measurements (1-minute resolution): feeder head power and node voltage magnitude. The relationship between the grid-level outputs and the home power is described by power flow equations. Here, we briefly introduce the linear power model [12] where the grid-level power and voltage magnitude are approximated as linear functions of home power injections:

$$\begin{bmatrix} P_0 \\ Q_0 \end{bmatrix} = H\Omega + e_0 \quad (2)$$

$$V_m = K\Omega + b + e_V \quad (3)$$

where $[P_0; Q_0] \in \mathbb{R}^{2 \times T}$ collects the feeder head real and reactive power; $V_m \in \mathbb{R}^{N \times T}$ is the bus voltage magnitudes; e_0 and e_V are the linear approximation errors. Coefficient matrices H , K , and b are provided next. Represent the system admittance matrix Y as

$$Y = \begin{bmatrix} Y_{00} & Y_{0L} \\ Y_{L0} & Y_{LL} \end{bmatrix} \in \mathbb{C}^{(N+1) \times (N+1)}. \quad (4)$$

Define $w := -Y_{LL}^{-1}Y_{L0}v_0$ as the zero-load voltage and let $W = \text{diag}(w)$. The coefficient matrices are given by:

$$H = [\mathcal{R}\{v_0 Y_{0L}^* M^*\}, \mathcal{I}\{v_0 Y_{0L}^* M^*\}] \quad (5)$$

$$K = |W| \mathcal{R}\{W^{-1} M\} \quad (6)$$

$$b = |w| \quad (7)$$

where the operator $*$ denotes the conjugate of a matrix, $\mathcal{R}\{\cdot\}$ and $\mathcal{I}\{\cdot\}$ are real and imaginary parts of a complex-valued matrix, and $M = [Y_{LL}^{-1}(W^*)^{-1}, -jY_{LL}^{-1}(W^*)^{-1}]$. See [12] for the derivation of (5)-(7).

Considering that PMU measurements are only available at a few feeder nodes, the voltage magnitude for a selected N^{sel} nodes is modeled as

$$V_m^{sel} = BV_m = B(K\Omega + b) + e_V^{sel}, \quad (8)$$

where $B \in \mathbb{R}^{N^{sel} \times N}$ is the submatrix of the $N \times N$ identity matrix by selecting the corresponding N^{sel} rows that have voltage measurements, and $e_V^{sel} = B e_V$.

III. HOME POWER MODELING

The home power injection Ω is modeled by the following components:

$$\Omega = -\Omega_1 - \Omega_2 + \Omega_3 + \varsigma \quad (9)$$

where $\Omega_1 \in \mathbb{R}^{2N \times T}$ represents sparse-switching loads, $\Omega_2 \in \mathbb{R}^{2N \times T}$ represents periodic loads, $\Omega_3 \in \mathbb{R}^{2N \times T}$ represents home PV generation, and $\varsigma \in \mathbb{R}^{2N \times T}$ is the modeling error. We next build mathematical models for these energy components.

A. Sparse-Switching Loads

The majority of residential loads have a switching behavior, including lighting devices, dishwashers, and electric vehicle chargers. When switched on or off, these loads maintain a nearly constant power consumption for a certain duration, resulting in sparse changes in their power consumption profile.

Denote $U \in \mathbb{R}^{T \times T}$ as the upper triangular matrix of all ones. We model the sparse switching loads as:

$$\Omega_1 = Z_1 U \quad (10)$$

where $Z_1 \in \mathbb{R}^{2N \times T}$ is a sparse matrix whose non-zero element $Z_1(i, t)$ captures the power change of home i at time t , indicating the switching activity of loads.

B. Periodic Loads

Residential homes have loads that switch periodically based on local conditions. One typical example is thermostatically controlled loads, like refrigerators and water heaters that switch from off to on, and vice versa, depending on the objects' temperature. If the surrounding environment remains the same, these loads will switch periodically to maintain a satisfactory quality of service.

To recover the power of periodic loads, we apply the discrete cosine transform to identify the frequencies of the

periodic loads. Let matrix $S \in \mathbb{R}^{T \times T}$ collect basis frequency components:

$$S := \begin{bmatrix} \phi(0,0) & \dots & \phi(0,T-1) \\ \vdots & \ddots & \vdots \\ \phi(T-1,0) & \dots & \phi(T-1,T-1) \end{bmatrix}$$

where

$$\phi(k,n) := \sqrt{\frac{1}{T}} \cos\left(\frac{\pi k(2n+1)}{2T}\right).$$

The power of periodic loads is modeled as the linear combination of cosine waves:

$$\Omega_2 = Z_2 S \quad (11)$$

where $Z_2 \in \mathbb{R}^{2N \times T}$ is a sparse matrix whose non-zero elements indicate the contribution of specific frequencies in home periodic loads.

C. Low-Rank PV Generation

PV generation is dependent on factors such as solar irradiance and weather conditions, which are commonly shared among neighboring homes. As a result, the PV power generation patterns in a neighborhood tend to be similar, suggesting the potential use of a low-rank matrix representation. Nuclear norm minimization is often used as a surrogate to find the minimum rank matrix. The nuclear norm is defined below:

$$\|L\|_* := \sum_i \sigma_i(L)$$

where $\sigma_i(L)$ is the i^{th} singular value of matrix L .

However, solving a large-size optimization problem with the nuclear norm is computationally intensive. In this case, we replace the low-rank matrix with a rank-one matrix, and accordingly, replace the nuclear norm with the L_2 norm. This rank-one matrix formulation is based on the assumption that all neighborhood PV generations follow the same pattern, but with different PV capacities. Hence, the residential PV power is modeled by:

$$\Omega_3 = \beta v^\top \quad (12)$$

where $v \in \mathbb{R}^T$ is the PV power basis for T time steps and $\beta \in \mathbb{R}^{2N}$ is the relative real and reactive PV power capacity of N homes. The vector β is assumed to be predetermined from customer reporting or historical PV data analysis.

D. Smart Meter Measurements

The smart meter measures the real and reactive power consumption of a home. Compared to grid PMUs, smart meters provide data at a relatively low time resolution. To integrate the home-level and grid-level data that are measured with different temporal resolutions, we employ the down-sampling technique [3]. Recall the PMU measuring interval is assumed to be 1 minute in Section II. Suppose the smart meter measuring interval is τ minutes, then $T_s := T/\tau$ is the number of smart meter measurements in T minutes, and each measurement is the average power over every τ minutes, i.e.,

$$\Omega_A := \Omega A \in \mathbb{R}^{2N_s \times T} \quad (13)$$

where the average operator $A := \frac{1}{\tau} \mathbf{I} \otimes \mathbf{1}$, in which, \otimes is the Kronecker product, $\mathbf{I} \in \mathbb{R}^{T_s \times T_s}$ is an identity matrix, and $\mathbf{1} \in \mathbb{R}^{\tau \times 1}$ is a column vector with all-one elements.

IV. POWER RECOVERY AND DISAGGREGATION

With the system data and models described in Sections II and III, the goal is to find the sparse matrices Z_1 and Z_2 , and the vector v so that the error between the model outputs and the measurement data is minimized. Therefore, the home power recovery problem is formulated below:

$$\begin{aligned} \underset{Z_1, Z_2, v}{\text{minimize}} \quad & \|\Omega_A - (-Z_1 U - Z_2 S + \beta v^\top) A\|_2 \\ & + \lambda_1 \|[P_0; Q_0] - H(-Z_1 U - Z_2 S + \beta v^\top)\|_2 \\ & + \lambda_2 \|V_m^{\text{sel}} - B(K(-Z_1 U - Z_2 S + \beta v^\top) + b)\|_2 \\ & + \lambda_3 \|Z_1\|_1 + \lambda_4 \|Z_2\|_1 + \lambda_5 \|v\|_2^2 + \lambda_6 \|Mv\|_2 \end{aligned} \quad (14a)$$

subject to

$$Z_1 U \geq 0, \quad Z_2 S \geq 0, \quad \beta v^\top \geq 0. \quad (14b)$$

The first three terms in the cost function (14a) minimize the modeling errors in the home power, the feeder head power, and the voltage magnitude at selected nodes, respectively. The remaining terms in (14a) are regularizers on the structures of the matrices used to disaggregate the home power. L_1 regularizations are used to promote the sparsity of matrices Z_1 and Z_2 ; and the squared L_2 norm is used to replace the nuclear norm regularization discussed in Section III-C. The last term promotes the smoothness of the PV power, where the matrix $M \in \mathbb{R}^{(T-1) \times T}$ is constructed to compute the temporal change in PV power, i.e.,

$$Mv = [v(2) - v(1), v(3) - v(2), \dots, v(T) - v(T-1)]^\top.$$

Weighting parameters λ_i , $i = 1, \dots, 6$ are used to balance different objectives in the cost function. Constraints (14b) are element-wise inequalities imposed to ensure non-negative load and PV power.

The solution to the problem (14) is then used to disaggregate the home power into three components: 1) $\Omega_1 = Z_1 U$ represents the sparse-switching loads; 2) $\Omega_2 = Z_2 S$ represents the periodic loads; and 3) $\Omega_3 = \beta v^\top$ represents the PV generation. In addition, the feeder-level disaggregation result is obtained using the linear power flow equation (2):

$$\Omega_1^{fh} = H\Omega_1, \quad \Omega_2^{fh} = H\Omega_2, \quad \Omega_3^{fh} = H\Omega_3, \quad (15)$$

where $\Omega_1^{fh} \in \mathbb{R}^{2 \times T}$, $\Omega_2^{fh} \in \mathbb{R}^{2 \times T}$, and $\Omega_3^{fh} \in \mathbb{R}^{2 \times T}$ are feeder-level components that represent the sparse-switching loads, periodic loads, and PV power, respectively.

V. NUMERICAL RESULTS

We conducted numerical studies on the 33-node distribution system [13] with real-world residential home datasets [14], where a typical summer day during the time period 6 am-8 pm was selected for demonstration. Fig. 1 shows the load and PV power of 6 home examples in the distribution system, and the net load is obtained as the difference between home load and

TABLE I
RESULTS WITH RESPECT TO VARIOUS SMART-METER RESOLUTIONS.

Smart meter resolution (minutes)	Recovery accuracy (1-NRMSE)					Sparsity rate	
	Feeder head power	Voltage magnitude	Home power	PV	Load	Z_1	Z_2
$\tau = 1$	92.62%	99.98%	88.38%	87.92%	79.02%	95.49%	95.89%
$\tau = 5$	89.35%	99.98%	84.50%	84.27%	73.96%	92.75%	96.29%
$\tau = 15$	86.38%	99.97%	79.35%	81.76%	67.67%	97.37%	93.53%
$\tau = 30$	81.11%	99.97%	73.21%	73.89%	59.7%	93.98%	95.96%

TABLE II
THE PERFORMANCE IS IMPROVED WITH ADDITIONAL VOLTAGE MEASUREMENTS.

Smart meter resolution ($\tau = 15$ minutes)	Recovery accuracy (1-NRMSE)					Sparsity rate	
	Feeder head power	Voltage magnitude	Home power	PV	Load	Z_1	Z_2
without voltage measurement	86.38%	99.97%	79.35%	81.76%	67.67%	97.37%	93.53%
with voltage measurement	97.14%	99.99%	84.64%	90.44%	76.23%	95.81%	92.77%

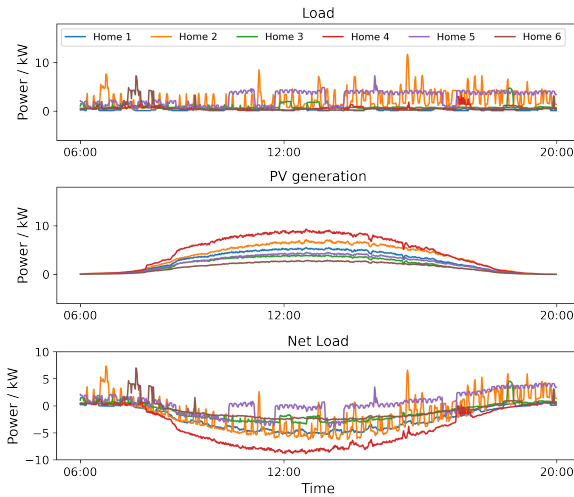


Fig. 1. Home power data with 1-minute resolution.

PV power ^{1,2}. The distribution system was simulated using pandapower [15], from where feeder head power and node voltages are obtained as PMU measurements.

We first present results with feeder head power data at 1-minute resolution and home power data at various resolutions of τ minutes. Results are summarized in Table I, where the recovery accuracy is quantified by 1 - NRMSE (normalized root mean squared error) and the matrix sparsity is quantified by the sparsity rate (percentage of zero elements in a matrix). Given the high sparsity rate shown in the last two columns, the power recovery accuracy is reasonably good, and the results can be further improved if we lower the matrix sparsity rate. It is worth noting that the voltage recovery is highly accurate as voltage changes in the system are small. Comparing rows in Table I, it is apparent that the recovery accuracy improves with the use of higher-resolution smart meter data.

¹Datasets [14] do not specify a load being sparse-switching or periodic, so there is no exact load component information and we plot the total load in the figure. For the same reason, we can only compute the overall load recovery error, as shown later in Tables I and II.

²For clarity, we only show the real power in all illustrating figures.

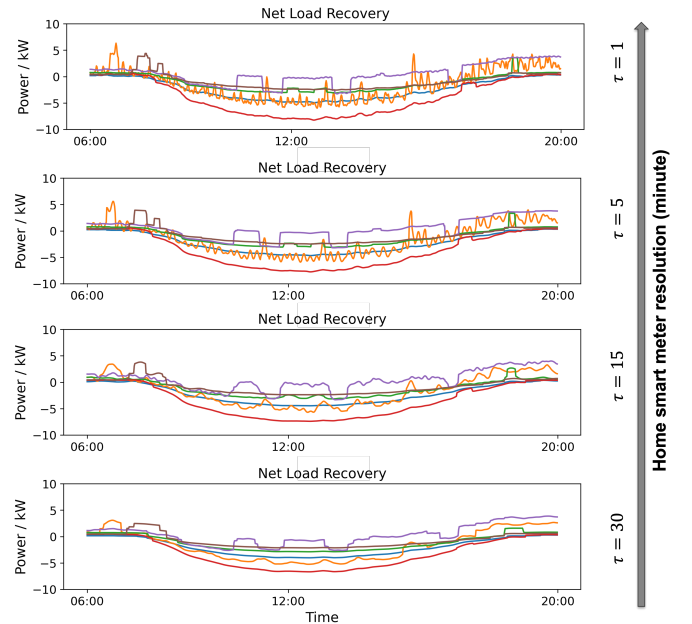


Fig. 2. The impact of the smart meter resolution on the net load recovery.

Fig. 2 shows the results of the net load recovery with respect to $\tau = 1, 5, 15,$ and 30 minutes. Comparison to the actual net load shown in Fig. 1 reveals that all results accurately capture the general power trend, and using higher-resolution smart meter data can lead to a more detailed recovery.

Leveraging voltage measurements

In this section, we evaluate the algorithm performance by adding voltage magnitude data of 1-minute resolution from nodes 5, 17, 21, 24, and 32 in the distribution network. The resolution of the smart meters data is assumed to be $\tau = 15$ minutes, in line with real-world applications. Table II compares disaggregation results with and without the voltage data, and it indicates the additional voltage data greatly improves the recovery accuracy, under similar matrix sparsity conditions.

The home power disaggregation results are depicted in Fig. 3. The top subplot presents the sparse switching loads

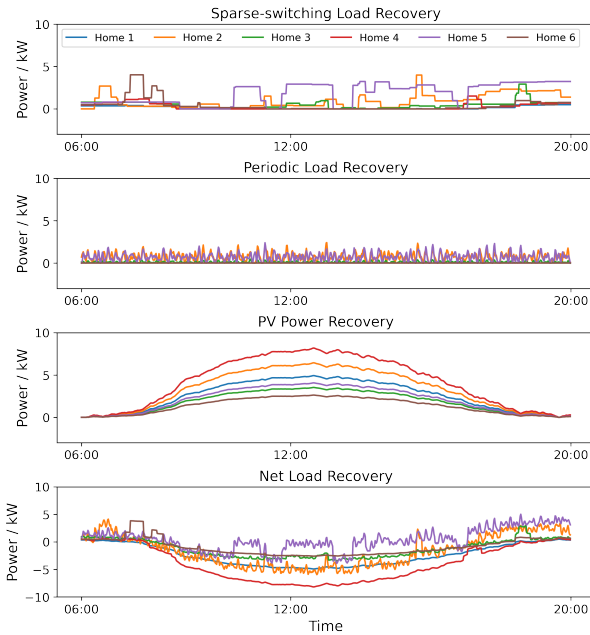


Fig. 3. Home power disaggregation results.

in homes, e.g., the purple-colored square wave is mainly contributed by the HVAC power in Home 5. The second subplot presents the home power of periodic loads, such as refrigerators and water heaters. The high-frequency components in the periodic load plots are partially caused by the noise term ς in the home power model (9). The third subplot represents the home PV power that was recovered using a rank-one matrix. The bottom subplot shows the home net load recovered by the rank-one matrix and matrices Z_1 and Z_2 with sparsity rates of 95.81% and 92.77%, respectively. Fig. 4 shows the power disaggregation results at the feeder head.

This information can assist grid operators monitoring and understanding the behaviors of different power components in the distribution system.

VI. CONCLUSIONS

This paper developed a power disaggregation algorithm to observe the residential power components within a feeder. We integrated the PMU and smart-meter data to recover the power of sparse-switching loads, periodic loads, and PV generation, at both home and feeder levels. The proposed algorithm is data efficient, benefiting from the preserved sparsity in matrix completion and the adoption of power system models. Numerical results using real-world residential data illustrate the efficacy of the proposed algorithm.

There are several promising avenues for future work. One is to develop a scalable framework that can handle large systems and high-resolution data, by using distributed algorithms. Another direction is to develop an online algorithm for real-time observation of feeder-level power components. Furthermore, exploring ways to leverage the disaggregation results to evaluate the system flexibility and support operations in bulk power systems could be a valuable research topic.

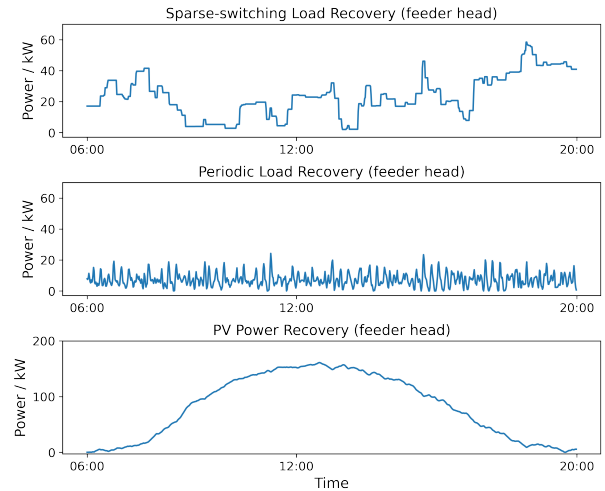


Fig. 4. Disaggregation results at the feeder head.

REFERENCES

- [1] S. Kaspour and A. Yassine, "A federated learning model with short sequence to point mechanism for smart home energy disaggregation," in *2022 IEEE Symposium on Computers and Communications (ISCC)*, 2022, pp. 1–6.
- [2] S. Zeinal-Kheiri, A. M. Shotorbani, and B. Mohammadi-Ivatloo, "Residential load disaggregation considering state transitions," *IEEE Transactions on Industrial Informatics*, vol. 16, no. 2, pp. 743–753, 2020.
- [3] S. Lin and H. Zhu, "Enhancing the spatio-temporal observability of grid-edge resources in distribution grids," *IEEE Transactions on Smart Grid*, vol. 12, no. 6, pp. 5434–5443, 2021.
- [4] X. Chen and O. Ardakanian, "Data efficient energy disaggregation with behind-the-meter energy resources," *Sustainable Energy, Grids and Networks*, vol. 32, p. 100813, 2022.
- [5] P. A. Schirmer and I. Mporas, "Non-intrusive load monitoring: A review," *IEEE Transactions on Smart Grid*, vol. 14, no. 1, pp. 769–784, 2023.
- [6] H. Kim, K. Ye, H. P. Lee, R. Hu, N. Lu, D. Wu, and P. Rehm, "An ica-based hvac load disaggregation method using smart meter data," 2022. [Online]. Available: <https://arxiv.org/abs/2209.09165>
- [7] E. C. Kara, C. M. Roberts, M. Tabone, L. Alvarez, D. S. Callaway, and E. M. Stewart, "Disaggregating solar generation from feeder-level measurements," *Sustainable Energy, Grids and Networks*, vol. 13, pp. 112–121, 2018.
- [8] G. S. Ledva and J. L. Mathieu, "Separating feeder demand into components using substation, feeder, and smart meter measurements," *IEEE Transactions on Smart Grid*, vol. 11, no. 4, pp. 3280–3290, 2020.
- [9] Y. Xu and J. V. Milanović, "Artificial-intelligence-based methodology for load disaggregation at bulk supply point," *IEEE Transactions on Power Systems*, vol. 30, no. 2, pp. 795–803, 2015.
- [10] D. Chakravorty, B. Chaudhuri, and S. Y. R. Hui, "Estimation of aggregate reserve with point-of-load voltage control," *IEEE Transactions on Smart Grid*, vol. 9, no. 5, pp. 4649–4658, 2018.
- [11] X.-Y. Zhang, C. Watkins, and S. Kuenzel, "Multi-quantile recurrent neural network for feeder-level probabilistic energy disaggregation considering roof-top solar energy," *Engineering Applications of Artificial Intelligence*, vol. 110, p. 104707, 2022.
- [12] A. Bernstein and E. Dall'Anese, "Linear power-flow models in multi-phase distribution networks," in *2017 IEEE PES Innovative Smart Grid Technologies Conference Europe (ISGT-Europe)*, 2017, pp. 1–6.
- [13] M. Baran and F. Wu, "Network reconfiguration in distribution systems for loss reduction and load balancing," *IEEE Transactions on Power Delivery*, vol. 4, no. 2, pp. 1401–1407, 1989.
- [14] Smart* data set for sustainability, University of Massachusetts Amherst. [Online]. Available: <http://traces.cs.umass.edu/index.php/Smart/Smart>
- [15] L. Thurner, A. Scheidler, F. Schäfer, J.-H. Menke, J. Dollichon, F. Meier, S. Meinecke, and M. Braun, "Pandapower—an open-source python tool for convenient modeling, analysis, and optimization of electric power systems," *IEEE Transactions on Power Systems*, vol. 33, no. 6, pp. 6510–6521, 2018.